Enhancing the Torque Density of Conventional PM-SynRel Machine with Hybrid Flux Barrier

R. M. Ram Kumar[†¶], Gaurang Vakil[†‡], David Gerada[†‡], Adam Walker[†], Salvatore La Rocca[†], Mahir Al-Ani[†], Chris Gerada[†‡], Krzysztof Paciura[§], Alastair McQueen[§] and B. G. Fernandes [¶]
[†] Power Electronics, Machines and Control Group, University of Nottingham, Nottingham NG7 2RD, U.K,
[‡] Ningbo 315000, China, [§] Cummins Corporate R&T, Peterborough, PE2 6FZ, U.K,
[¶] Department of Electrical Engineering, Indian Institute of Technology - Bombay, Powai, Mumbai - 400076, India
Email: ramkumar.ramanathan@nottingham.ac.uk, gaurang.vakil@nottingham.ac.uk

***Abstract*—Electrical machines with high torque density are required for traction application. Availability of bonded magnets with complex shapes and magnetization pattern can significantly extend the design space of electrical machines. This paper introduces a hybrid flux barriers design to improve the torque density of permanent magnet assisted synchronous reluctance (PM-SynRel) machine using ferrite magnets. The torque density with hybrid flux barriers is found to improve along the entire range of speed compared to the conventional flux barriers. The hybrid barrier design achieves similar performance to that of curved barrier with relatively flat shaped magnets in the last flux barrier. Thus, the hybrid barrier is able to enhance the torque density at a potentially reduced cost of manufacturing. The hybrid flux barrier design is validated for both electromagnetic and mechanical performance using commercial finite element analysis (FEA) packages.**

***Index Terms*—High torque density, hybrid barrier, ferrite magnets, bonded magnets**

I. Introduction

The fuel economy of an electric vehicle (EV) is significantly influenced by its curb weight. The city fuel economy of an EV decreases by the increase in curb weight compared to the highway fuel economy [1]. The duration of high way operation constitutes a small fraction of its running time for most of the EVs. Hence, curb weight reduction should be addressed during the design of various sub components in an EV. Curb weight can be reduced by integrating components together and secondly increasing the power sensity of individual components, i.e. electric machine, inverter, battery, etc as well [2]. The mass of an electric machine can be reduced by increasing its torque and power density. For a fixed cooling system, the maximum achievable power density is curtailed by the choice of gear box and the rotor dimensions. Any further reduction in the mass of an electric machine can be realized by only increasing its torque density.

PM-SynRel machine has been subjected to extensive research for traction application due to its inherent advantages like reduced use of PM, high constant power speed range, high torque per ampere, etc [3]. The PM-SynRel machine with rare earth magnets are used in BMW i3 and i8 [4]. High torque density can be quite easily achieved even with conventional design for a PM-SynRel with rare earth magnets. However, automakers are focused in reducing the content of rare earth magnets in electric machines used in EVs. Another field of interest is in the replacement of rare earth magnets with ferrite magnets [5]. In order to achieve similar performance as rare earth magnets, the volume of ferrite PM required is high and conventional designs with magnets at the center of the flux barrier finds it difficult to house the huge volume of magnets. This necessitates filling the entire barrier with PMs and also demands for investigating alternative flux barrier shapes to increase the torque.

In the past, PMs were available only with rectangular or circular cross sections. It is difficult to fabricate complex shapes in case of sintered magnets. This limitation on the geometry of PM decreased the design space of flux barrier shapes in PM-SynRel machines. The section of flux barriers which hold the PM is either rectangular or circular in cross section. However, with the advent of bonded magnets, complex shapes and magnetization are easy to implement. Therefore, alternate flux barrier shapes can be investigated without being constrained by the shape of PMs [6].

Improving the electromagnetic performance especially in terms of reduced torque ripple has been the prime subject of research while analyzing alternate geometry for flux barriers. These are implemented in low power low speed machines where torque ripple minimization is essential for achieving better performance. However, high power and high speed electric machines are the future trends in traction application [7]. These high power high speed traction machines have significant mechanical stress. Therefore, it becomes essential to optimize the shape of flux barrier and hence the PMs considering both mechanical and electromagnetic performance.

This paper will discuss the various shapes of flux barrier

TABLE I
Target specifications of the machine

Rated Speed (rpm)	4500
Rated Torque (Nm)	400
Maximum Speed (rpm)	15000
Torque at maximum speed (Nm)	150
DC Bus voltage (V)	600 V

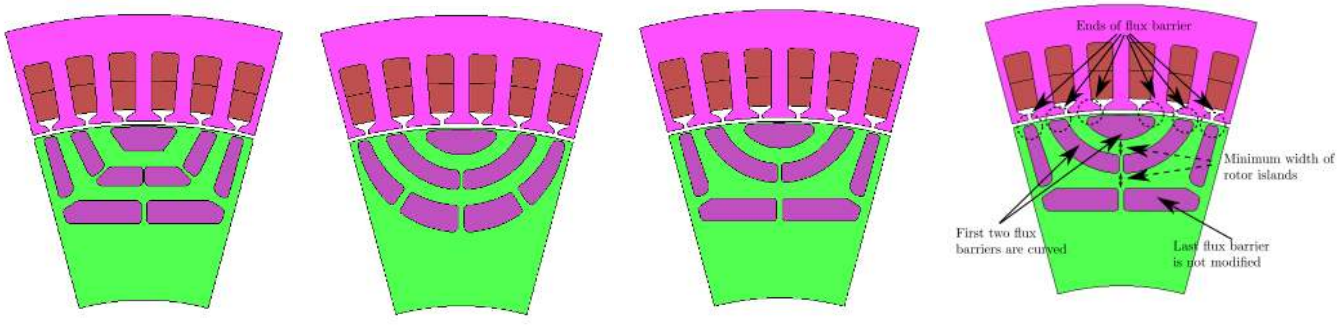

(a) (b) (c) (d)

Fig. 1. Types of flux barriers in PM-SynRel (a) Conventional flux barrier (b) Curved flux barrier (c) Hybrid flux barrier (d) Hybrid flux barrier derived from conventional flux barrier

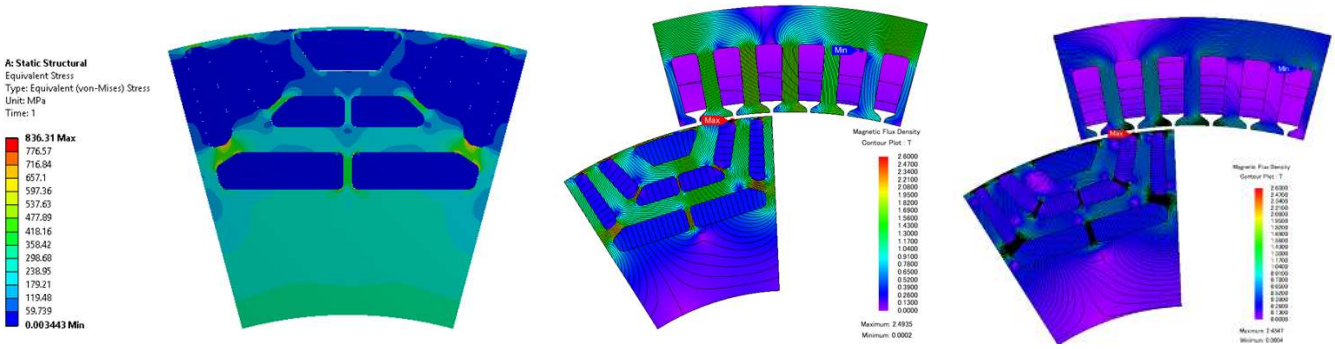

(a) (b) (c)

Fig. 2. Simulation results of conventional flux barrier design (a) Von Mises stress (b) Flux density at rated speed (c) Flux density at maximum speed

presented in literature for a PM-SynRel machine. The subsequent section will clarify the requirement of a hybrid flux barrier. The final section will introduce a hybrid flux barrier and compare its performance with the curved flux barrier at both rated and high speed operations.

II. Design of PM-SynRel Machine with Conventional Flux Barrier

The PM-SynRel with conventional flux barrier is derived by filling the flux barriers of conventional SynRel machine with PMs as shown in Fig. 1(a). The flux barriers of conventional SynRel machines are nearly rectangular in cross section. The torque requirement of the PM-SynRel machine at both rated and maximum speed is listed in Table I. The machine is designed for a peripheral speed of 175 m/s. Since the peripheral speed is in excess of 150 m/s, this machine belongs to the category of high power high speed machine [8].

The design of conventional PM-SynRel machine is performed by only considering the torque requirements. The position of the ends of flux barrier as shown in Fig. 1(d), highly influences the torque ripple of SynRel machine. As torque enhancement is the basic design objective, the effect of flux barrier ends on torque ripple will be analyzed after identifying suitable barrier shape using the average torque. Based on this, a 12 pole PM-SynRel machine with equally spaced flux barrier ends is designed. The main dimensions of the machine like stack length, rotor outer diameter, air gap length and stator outer diameter are 220 mm, 222 mm, 1 mm and 280 mm respectively. Compared to the conventional SynRel machine, the only notable difference is the absence of iron island closer to the airgap. The iron island comprises of the rotor lamination which is denser compared to the ferrite PM. Hence, replacing the iron island closer to the airgap with ferrite PM will reduce the mechanically induced stress in rotor.

TABLE II
Performance of Conventional Flux Barrier

	Torque (Nm)	Torque ripple (%)
Rated Speed	420.3	17.7
Maximum Speed	155.33	47.64

The electromagnetic performance of the conventional PM-SynRel machine is shown in Table II. The machine is found to satisfy the requirements listed in Table I. The torque ripple of the machine is quite high due to equispaced flux barrier ends. This can be significantly reduced by optimizing the ends of flux barrier and also by skewing the rotor. The flux density plots at rated and maximum speed of operation are shown in Figs. 2(b) and 2(c). The flux density in the core is found to be significantly less at maximum speed due to field weakening. The Von-Mises stress is obtained at 16,500 rpm by considering a safety factor of 10% on the maximum speed. It can be observed that the maximum Von-Mises stress is around 836

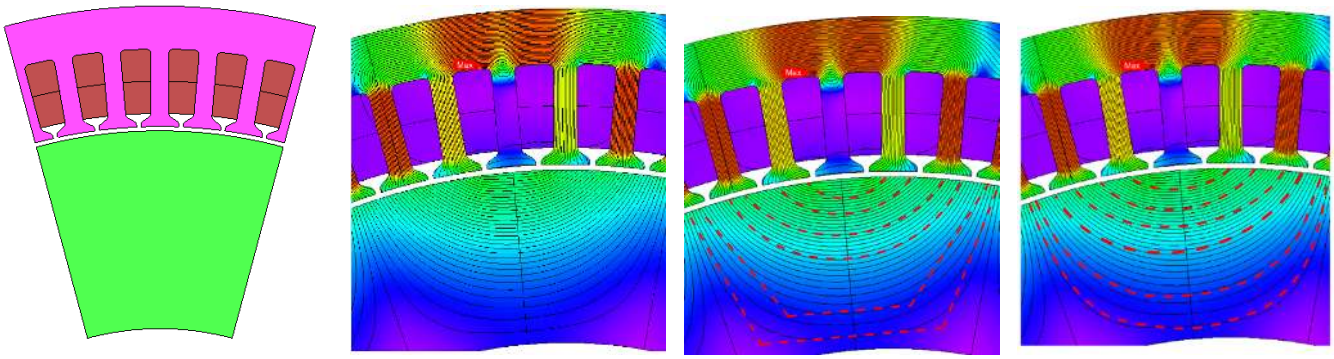

(a) (b) (c) (d)

Fig. 3. Simulation plots showing (a) cylindrical rotor without flux barrier (b) No load flux lines (c) Approximation to hybrid flux barrier (d) Approximation to curved flux barrier

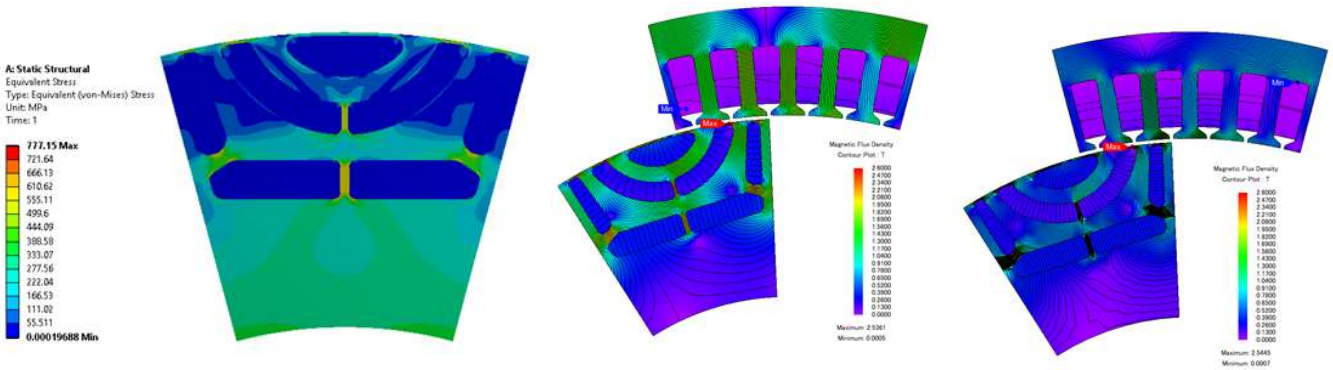

(a) (b) (c)

Fig. 4. Simulation results of hybrid flux barrier derived from conventional flux barrier showing (a) Von Mises stress (b) Flux density at rated speed (c) Flux density at maximum speed

MPa which is below the yield limit of 35HXT780T (i.e 850 MPa) used for the rotor core. Therefore, the conventional PM-SynRel machine satisfies both electromagnetic and mechanical requirements. This will be used as a bench mark design for further studies.

III. Need for Hybrid Flux Barrier design

The various shapes of flux barriers and corresponding magnets proposed in literature can be classified into the following categories: conventional with flat magnets [9], curved with curved magnets [10] [11], asymmetric rotor with flat magnets [12] and flux barriers curved to the shape of flux lines with flat magnets. The three flux barriers in each of the aforementioned designs are of the same shape. The design of flux barriers according to the shape of flux lines is specifically proposed in literature to improve the torque and power factor [13]. This is achieved by improving the d-axis inductance and reducing the q-axis inductance or in other words improving the reluctance torque component of the machine. Improved power factor and reluctance torque are very much essential in case of traction machine. High reluctance torque enables to reduce the content of PMs while a good power factor can improve the driving range of the vehicle. However, shaping the flux barriers according to flux lines increases the tooling cost while manufacturing PMs with the same shape. Cost is another dominating factor in automobile industry. Therefore, the main objective of this research aims at improving the shape of flux barrier by giving due consideration to the PMs.

TABLE III
Performance of hybrid flux barrier derived from conventional flux barrier

	Torque (Nm)	Torque ripple (%)
Rated Speed	435.38	19.33
Maximum Speed	167.76	47.69

The no load flux lines are shown in Fig. 3(b). These flux lines are obtained using a cylindrical rotor without flux barriers as shown in Fig. 3(a). The flux lines tend to take a curved shape in the rotor to have minimum reluctance. However, the degree of the curvature of flux lines closer to the airgap is more compared to the ones closer to the shaft. In this section, analysis is performed considering the shape of first two flux barriers closer to airgap. The next section will improve on these results by analyzing the shape of third flux barrier.

The first two flux barriers of the conventional design are modified to curved barriers while the third barrier is left undisturbed as shown in Fig. 1(d). This results in the derived hybrid barrier shown in Fig. 1(c). In order to ensure a fair comparison the following factors are maintained same in conventional and hybrid flux barrier designs : the volume of

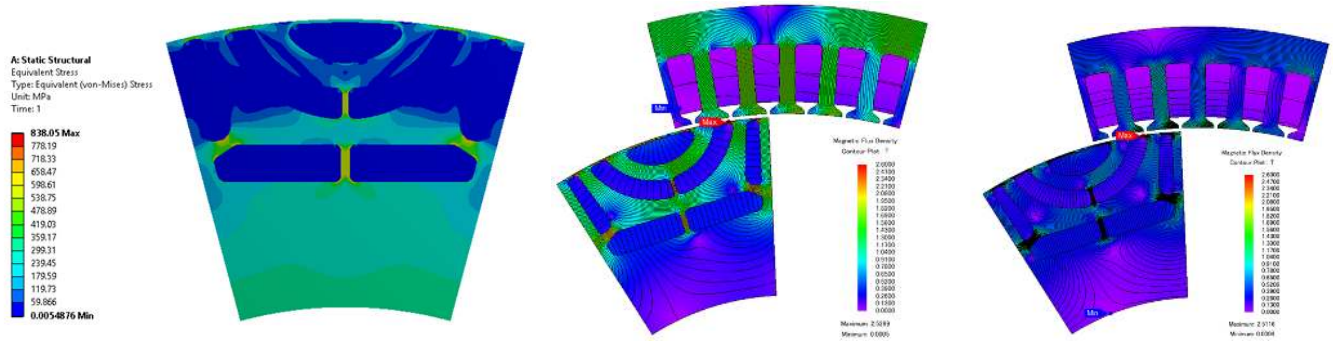

(a) (b) (c)

Fig. 5. Simulation results of hybrid flux barrier showing (a) Von Mises stress (b) Flux density at rated speed (c) Flux density at maximum speed

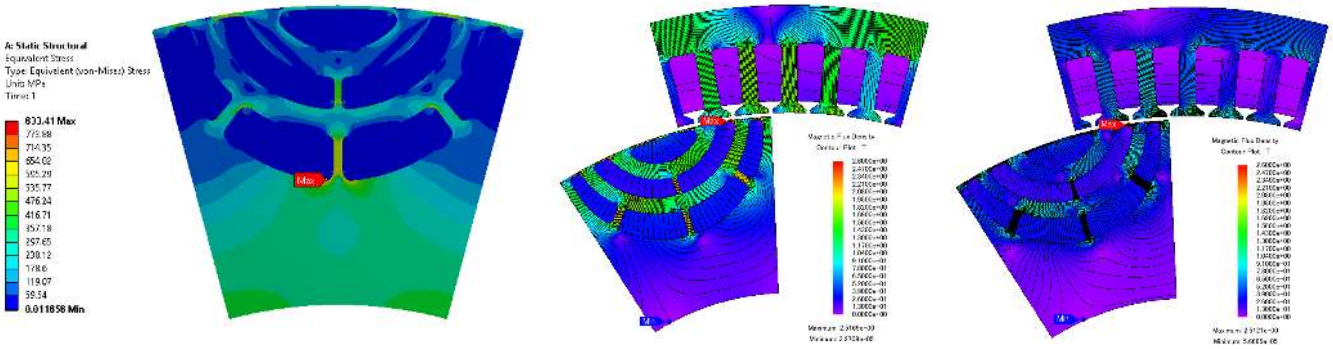

(a) (b) (c)

Fig. 6. Simulation results of curved flux barrier showing (a) Von Mises stress (b) Flux density at rated speed (c) Flux density at maximum speed

TABLE IV
COMPARISON OF HYBRID AND CURVED FLUX BARRIER

	Hybrid	Curved
Torque at rated Speed (Nm)	442.7	440.7
Torque ripple at rated Speed (%)	20.69	20.19
Copper loss at rated speed (kW)	0.47	0.467
Iron loss at rated speed (kW)	2.284	2.178
Efficiency at rated speed (%)	98.82	98.86
Torque at maximum Speed (Nm)	175.15	175.1
Torque ripple at maximum Speed (%)	53.38	50.5
Copper loss at maximum speed (kW)	1.138	1.095
Iron loss at maximum speed (kW)	5.046	4.876
Efficiency at maximum speed (%)	97.8	97.87

PM in each flux barrier, the position of flux barrier ends, minimum width of rotor islands as shown in Fig. 1(d). This results in nearly same contribution by PMs to the total torque, same torque ripple and maximum saturation of rotor islands.

The maximum value of Von Mises stress for the derived hybrid rotor as shown in Fig. 4(a) is nearly 777 MPa. A further improvement in performance is possible by reducing the iron rib thickness as the value of maximum stress is much below the yield limit of 850 MPa. The flux density plots at rated and maximum speed of operation are shown in Figs. 4(b) and 4(c) respectively. The electromagnetic performance in terms of average torque and torque ripple is listed in Table III for the machine with derived hybrid flux barrier. The hybrid rotor derived from conventional flux barrier is found to provide 3.58% and 8% more torque at rated and maximum speed compared to the bench mark design shown in Table II. The average torque improves by nearly the same magnitude at both rated and maximum speed of operation. This can be interpreted as the entire torque speed characteristics of the machine shifting up vertically. The improvement in average torque is obtained without a significant change in the torque ripple. This validates the need for first two flux barriers to be curved in shape. The next section will analyze the shape of the third layer of flux barrier.

IV. COMPARISON BETWEEN HYBRID AND CURVED FLUX BARRIER

The two types of flux barrier approximation based on the no load flux lines are given in Figs. 3(c) and 3(d). In both cases the first two flux barriers are curved in shape. However, the third barrier can be approximated to either curved or conventional flux barrier. This results in two different rotor structures, namely curved and hybrid flux barriers. The structure of curved and hybrid barriers are shown in Figs. 1(b) and 1(c) respectively. Chevrolet Volt uses the curved barrier with ferrite magnets, where the PMs are arc shaped and magnets in the third flux barrier are maintained to be the same size to reduce the tooling cost [14].

In order to ensure a fair comparison, both hybrid and curved flux barrier PM-SYnRel machines are designed for same volume of PM in each layer, position of flux barrier ends and minimum width of rotor islands as mentioned in

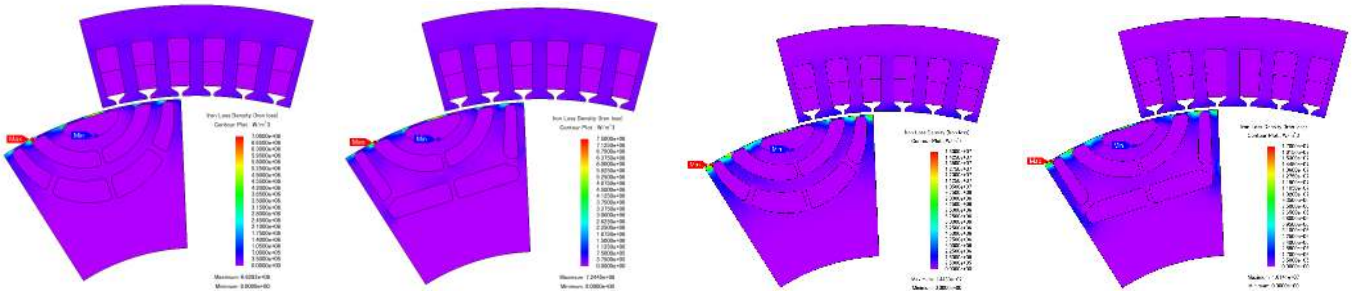

(a) (b) (c) (d)

Fig. 7. Simulation results showing the iron loss density (a) Curved flux barrier at rated speed (b) Hybrid flux barrier at rated speed (c) Curved flux barrier at maximum speed (d) Hybrid flux barrier at maximum speed

the previous section. The simulation results for hybrid and curved flux barriers are shown in Figs. 5 and 6 respectively. The maximum value of Von Mises stress is nearly 838 MPa and 833 MPa in hybrid and curved flux barrier as shown in Figs. 5(a) and 6(a) respectively. This justifies that both the rotor structures are equally stressed from the mechanical considerations. The flux density plots for hybrid flux barrier at rated and maximum speed of operation are shown in Figs. 5(b) and 5(c) respectively. Similarly, the flux density plots for curved flux barrier at rated and maximum speed of operation are shown in Figs. 6(b) and 6(c) respectively.

The electromagnetic performance of both the machines are listed in Table IV. The parameters of interest for EVs like torque, torque ripple and efficiency are chosen for comparison. For both hybrid and curved flux barrier, the angle of advance of current for maximum torque per ampere at rated speed is found to be the same. The angle of advance is also same during the field weakening operation at maximum speed. The average torque and torque ripple of both machines are nearly same at both rated and maximum speed. The torque ripple is significantly high in both hybrid and curved barrier. However, this can be reduced by optimizing the position of flux barrier ends and skewing the rotor. Therefore, the torque ripple is used here just a parameter of comparison for a particular position of flux barrier ends.

The iron loss, copper loss and the efficiency of both machines are given in Table IV. There is no significant effects on these quantities by the shape of the third flux barrier. The iron loss is obtained by assuming a build factor of 2. The iron loss density plots for curved flux barrier at rated and maximum speed of operation are shown in Figs. 7(a) and 7(c) respectively. Similarly, the iron loss density plots for hybrid flux barrier at rated and maximum speed of operation are shown in Figs. 7(b) and 7(d) respectively. The iron loss density is of the same order of magnitude at both rated and maximum speed for both hybrid and curved flux barrier. The efficiency is calculated by considering only the dc copper loss and iron loss. Therefore, the efficiency reported here can be used for comparison but cannot be considered as a result of exhaustive analysis.

Another important factor of concern in PM-SynRel machine with ferrite magnets is the risk of demagnetization. The

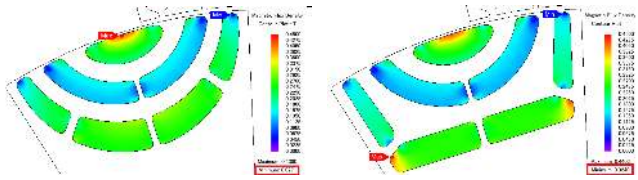

(a) (b)

Fig. 8. Simulation results showing the operating point of PM with only demagnetizing current at maximum speed for (a) Curved flux barrier (b) Hybrid flux barrier

ferrite magnets are low energy magnets and their coercivity decreases with increase in temperature. The traction motors are found to operate at temperatures in excess of 100°C. The simulations are performed by assuming an operating temperature of 100°C for the ferrite magnets (FB13B). This grade of PM does not have the knee point in second quadrant at 100°C. Therefore, operating point above a flux density of 0 T can prevent the magnet from irreversible demagnetization. The demagnetization studies are performed by considering a fully demagnetizing current of about 1.5 times the rated current at maximum speed. The results of the demagnetization studies are shown in Fig. 8 by highlighting the minimum value of flux density. The value of minimum operating point of PMs is above 0 T for both hybrid and curved flux barrier designs. Hence, the magnets are not subjected to irreversible demagnetization.

The performance of curved and hybrid flux barriers are found to be very similar based on the all above mentioned criteria. The third flux barrier in case of the hybrid flux barrier houses magnets which are nearly rectangular in cross section. It is relatively easy to fabricate and magnetize rectangular magnets compared to curved magnets. In addition to this, the third flux barrier houses the maximum volume of PMs. Therefore, hybrid flux barrier can provide similar performance to that of curved flux barrier at reduced cost of fabrication.

V. Effect of Flux Barrier Ends on Torque Ripple

In the previous section the performance of hybrid and curved flux barrier were compared by analyzing the performance of one particular geometry. However, in order to arrive at an unambiguous conclusion, it would be beneficial to compare hybrid and curved flux barrier with another set of

TABLE V
COMPARISON OF HYBRID AND CURVED FLUX BARRIER WITH A DIFFERENT POSITION OF THIRD FLUX BARRIER ENDS

	Hybrid	Curved
Torque at rated Speed (Nm)	438.27	437.85
Torque ripple at rated Speed (%)	17.68	16.67
Torque at maximum Speed (Nm)	156.99	159.34
Torque ripple at maximum Speed (%)	23.56	22

geometrical parameters. The main drawback of the geometry considered in the previous section was its high torque ripple. The torque ripple of a PM-SynRel machine is a complex function of flux barriers ends [15]. Therefore, this section analyzes the optimization of flux barrier ends to reduce the torque ripple.

The first two flux barriers are common in both hybrid and curved flux barrier machines. Hence, varying the position of the ends of last flux barrier will result in a better understanding of the rotor geometries. Based on this the position of the third flux barrier ends are increased by 0.5° w.r.t the axis of PM. The resulting electromagnetic performance of both hybrid and curved flux barrier PM-SynRel after changing the flux barrier ends is shown in Table V. It can be observed that, there is a reduction in both average torque and the torque ripple. However, the reduction in torque ripple especially at maximum speed from nearly 50% to 22% is more evident compared to the decrease in torque ripple at rated speed. Though the average torque also reduces, it is sufficient enough to satisfy the design requirements mentioned in Table I.

On comparing Table IV and V, the change in the position of the third flux barrier end reflects the same way on torque and torque ripple in both hybrid and curved flux barrier PM-SynRel. In addition to that, the performance for both hybrid and curved flux barrier with modified flux barrier end is found to be very similar as listed in Table V. Further reduction in torque ripple can be achieved by optimizing all the flux barrier ends over the entire design space. The aforementioned observations, proves that the modification in shape of the last flux barrier from curved to conventional does not effect the performance of the PM-SynRel machine.

VI. CONCLUSION

PM-SynRel machine with hybrid flux barrier is proposed in this paper. High power high speed machines based on conventional, hybrid and curved flux barrier are designed considering both electromagnetic and mechanical performance. The important observation on comparing the performance of these designs are listed below :

- Curved and hybrid flux barrier PM-SynRel are found to exhibit better performance in terms of average torque compared to the conventional PM-SynRel.
- Curved and hybrid flux barrier PM-SynRel show similar performance in terms of average torque, torque ripple and efficiency.
- PM-SynRel with hybrid flux barrier uses flat magnets with nearly rectangular cross section in the third flux barrier. The fabrication and magnetization of rectangular magnets are easy compared to curved magnets.
- The superior performance of curved flux barrier can be realized using hybrid flux barrier at reduced cost of PM fabrication as the cost of fabrication plays an important role in automobile industry.
- The number of curved magnets per pole is reduced from 7 to 3 on moving from curved to hybrid flux barrier PM-SynRel The relatively flat magnets occupy the last flux barrier and share a major fraction of total PM by volume.

REFERENCES

[1] H. Jung, R. Silva, and M. Han, "Scaling Trends of Electric Vehicle Performance: Driving Range, Fuel Economy, Peak Power Output, and Temperature Effect," World Electric Vehicle Journal, 9(4), 46, 2018.

[2] T. Burress and S. Campbell, "Benchmarking EV and HEV power electronics and electric machines," 2013 IEEE Transportation Electrification Conference and Expo (ITEC), Detroit, MI, 2013, pp. 1-6.

[3] N. Bianchi, S. Bolognani, E. Carraro, M. Castiello and E. Fornasiero, "Electric Vehicle Traction Based on Synchronous Reluctance Motors," IEEE Transactions on Industry Applications, vol. 52, no. 6, pp. 4762-4769, Nov.-Dec. 2016.

[4] J. Merwerth, "The hybrid-synchronous machine of the new BMW i3 & i8 challenges with electric traction drives for vehicle, BMW Group," Workshop Lund University, 2014.

[5] "The Roadmap Report Towards 2040: A Guide to Automotive Propulsion Technologies," Advanced Propulsion Centre UK, 2018.

[6] E. Poskovic, C. Babetto, N. Bianchi and L. Ferraris, "The study of permanent magnet assisted reluctance machine with the adoption of NdF eB bonded magnets," 2018 International Symposium on Power Electronics, Electrical Drives, Automation and Motion (SPEEDAM), Amalfi, 2018, pp. 274-279.

[7] D. Golovanov, L. Papini, D. Gerada, Z. Xu and C. Gerada, "Multidomain Optimization of High-Power-Density PM Electrical Machines for System Architecture Selection,"IEEE Transactions on Industrial Electronics, vol. 65, no. 7, pp. 5302-5312, July 2018.

[8] D. Gerada, A. Mebarki, N. L. Brown, C. Gerada, A. Cavagnino and A. Boglietti, "High-Speed Electrical Machines: Technologies, Trends, and Developments," IEEE Transactions on Industrial Electronics, vol. 61, no. 6, pp. 2946-2959, June 2014.

[9] Y. Kong, M. Lin, M. Yin and L. Hao, "Rotor Structure on Reducing Demagnetization of Magnet and Torque Ripple in a PMa-synRM With Ferrite Permanent Magnet," in IEEE Transactions on Magnetics, vol. 54, no. 11, pp. 1-5, Nov. 2018, Art no. 8108705.

[10] H. Huang, Y. Hu, Y. Xiao and H. Lyu, "Research of Parameters and Antidemagnetization of Rare-Earth-Less Permanent Magnet-Assisted Synchronous Reluctance Motor," in IEEE Transactions on Magnetics, vol. 51, no. 11, pp. 1-4, Nov. 2015, Art no. 8112504.

[11] W. Zhao, F. Xing, X. Wang, T. A. Lipo and B. Kwon, "Design and Analysis of a Novel PM-Assisted Synchronous Reluctance Machine With Axially Integrated Magnets by the Finite-Element Method," in IEEE Transactions on Magnetics, vol. 53, no. 6, pp. 1-4, June 2017, Art no. 8104104.

[12] W. Zhao, D. Chen, T. A. Lipo and B. Kwon, "Performance Improvement of Ferrite-Assisted Synchronous Reluctance Machines Using Asymmetrical Rotor Configurations," in IEEE Transactions on Magnetics, vol. 51, no. 11, pp. 1-4, Nov. 2015, Art no. 8108504.

[13] Y. Wang, G. Bacco and N. Bianchi, "Geometry analysis and optimization of PM-assisted reluctance motors," 2016 XXII International Conference on Electrical Machines (ICEM), Lausanne, 2016, pp. 1756-1762.

[14] S. Jurkovic, K. Rahman, N. Patel, and P. Savagian, "Next generation voltec electric machines; design and optimization for performance and rare-earth mitigation," SAE International Journal of Alternative Powertrains, 4(2), 336-342.

[15] N. Bianchi, S. Bolognani, D. Bon and M. Dai Pr, "Torque Harmonic Compensation in a Synchronous Reluctance Motor," in IEEE Transactions on Energy Conversion, vol. 23, no. 2, pp. 466-473, June 2008.